


## Trap-Free Space-Charge-Limited Hole Transport in a Fullerene Derivative

N.B. Kotadiya, P.W.M. Blom, and G.A.H. Wetzelaer\*

Max Planck Institute for Polymer Research, Ackermannweg 10, 55128 Mainz, Germany

 (Received 17 August 2018; revised manuscript received 13 December 2018; published 27 February 2019)

Fullerenes and their derivatives are well-known electron-transporting materials used in organic solar cells and transistors. However, the extent to which fullerenes are able to transport holes is heavily disputed. Using selective Ohmic contacts, we study the bulk hole and electron transport in a bisadduct fullerene derivative. Trap-free space-charge-limited hole and electron currents are measured, with a hole mobility equivalent to the electron mobility. Our results identify the bisadduct fullerene as an organic semiconductor with balanced bipolar bulk transport with excellent electron and hole mobilities.

DOI: [10.1103/PhysRevApplied.11.024069](https://doi.org/10.1103/PhysRevApplied.11.024069)

Fullerenes and their derivatives are widely used in organic solar cells, in  $n$ -channel transistors, and as  $n$ -type thermoelectric materials, owing to their excellent electron-transport capabilities [1,2]. For the same reason, fullerenes have been successfully applied as electron-transport layers in hybrid perovskite photovoltaic cells [3]. By functionalizing fullerenes, such as  $C_{60}$  and  $C_{70}$ , with side groups, their solubility and energy levels can be tuned, enabling their use in solution-processed electronic devices [4–6].

With regard to electron transport, fullerenes exhibit mobilities that are among the highest in organic semiconductors [7] and exceptionally long electron diffusion lengths have recently been observed [8]. The electron-transporting character of fullerenes has led to their classification as “ $n$ -type” materials [1], though it has been shown that films of  $C_{60}$  can also support radical cations [9]. The extent to which fullerenes are able to transport holes, on the other hand, is less clear. From a theoretical perspective, the intrinsic electron and hole mobilities are comparable in many organic semiconductors [10], which would also be expected to hold for fullerenes. However, experimentally, unipolar charge transport is often observed in organic semiconductors due to charge trapping [11,12].

Evidence of a balanced electron and hole mobility in fullerenes has been reported for vapor-phase-grown  $C_{60}$  single crystals, measured with the photocurrent time-of-flight technique [13]. However, deep trapping sites for holes were also observed, which have negligible influence on the measured transit time [14], but can greatly hinder steady-state charge transport. In films of  $C_{60}$ , the hole mobility has been reported to be many orders of magnitude lower than the electron mobility [15–17]. In later work, a field-effect transistor using a solution-processed layer of the fullerene derivative [60][6,6]-phenyl  $C_{61}$  butyric

acid methyl ester (PCBM) was fabricated, exhibiting balanced electron and hole mobilities at high gate bias [18]. However, at low gate bias, a very low hole current was observed, which was ascribed to the presence of a large hole-injection barrier. In a field-effect transistor at high gate bias, charge-carrier densities are high, which obscures the presence of bulk traps or tail states to a certain degree [19]. By contrast, at low carrier densities in a diode configuration, measurements of the bulk mobility in [60]PCBM and [70]PCBM showed highly unipolar transport, with hole mobilities more than six-orders of magnitude lower than the electron mobilities [20], comparable to what has been observed for  $C_{60}$  thin films [15–17]. It should be noted that for charge-transport characterization in a diode configuration, Ohmic contacts are of critical importance.

In this article, we demonstrate trap-free space-charge-limited hole and electron currents in diodes based on a solution-processed bisadduct fullerene derivative. The bulk hole and electron mobilities are balanced and both are higher than  $10^{-3}$   $\text{cm}^2/\text{V s}$ . Numerical modeling of the current-density voltage characteristics shows that the energetic disorder for holes and electrons is similar. These measurements demonstrate that fullerenes can be excellent hole-transporting materials. The absence of charge trapping for both types of charge carriers reveals the intrinsic bipolar character of charge transport in organic semiconductors, as would be theoretically expected, but is rarely observed experimentally.

For our charge-transport measurements, the fullerene derivative indene- $C_{60}$  bisadduct (ICBA) is chosen (Fig. 1). ICBA is a bisadduct fullerene, exhibiting a highest occupied molecular orbital (HOMO) and lowest unoccupied molecular orbital (LUMO) that are raised by 0.2 eV as compared to PCBM [7]. The shallower HOMO (–5.9 eV) is expected to alleviate hole-injection issues, and should allow for Ohmic hole-contact formation using a recently developed technique [21]. Hole-only devices

\*wetzelaer@mpip-mainz.mpg.de

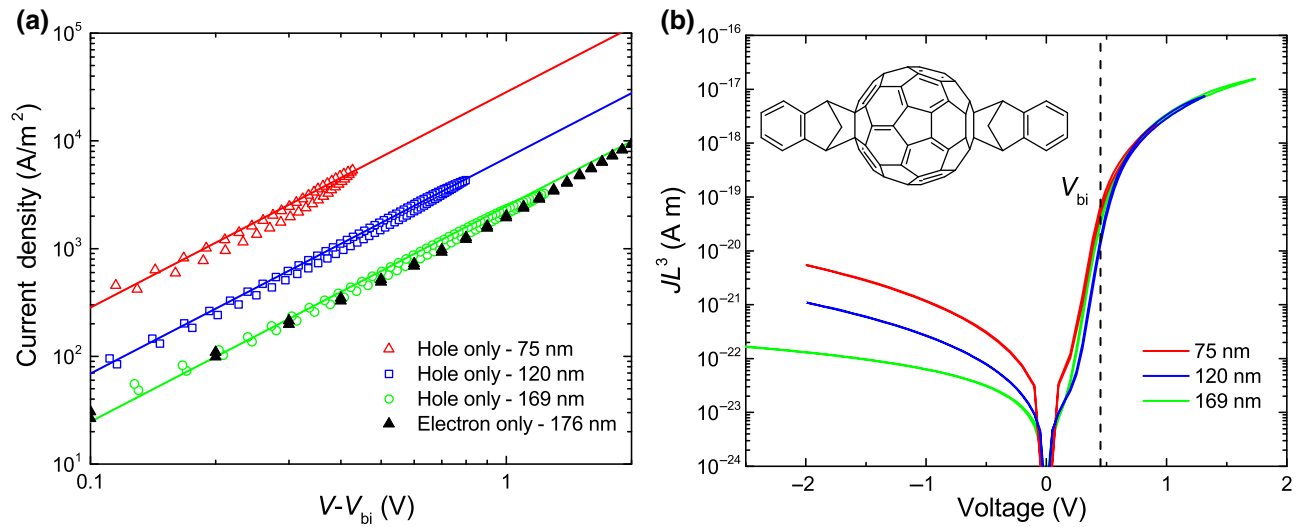


FIG. 1. (a) Current density-voltage characteristics of ICBA single-carrier devices. Hole-only devices of different layer thicknesses are shown (open symbols), with the voltage corrected for the built-in voltage (0.40–0.45 V) and the electrode series resistance. The solid lines are fits with Eq. (1), using a mobility of  $3 \times 10^{-3} \text{ cm}^2/\text{V s}$  for all layer thicknesses. A 176-nm-thick electron-only device is plotted for comparison (closed symbols). The error (standard deviation) in the thickness is determined to be 3–4 nm for all films. (b) Thickness-scaled current density ( $JL^3$ ) vs voltage for ICBA hole-only devices. The built-in voltage, which marks the transition from the exponential diffusion regime to the quadratic drift regime, is indicated by the dashed line at 0.45 V. The chemical structure of ICBA is shown in the inset.

are prepared, with ICBA spin coated from a chloroform solution on top of glass substrates with patterned indium-tin-oxide electrodes, covered with a 40-nm layer of poly(3,4-ethylenedioxythiophene)-poly(styrenesulfonate) (PEDOT:PSS), which has a work function of approximately 5.2 eV. To establish an Ohmic hole contact, a top electrode comprising  $\text{C}_{60}$ (4 nm)/ $\text{MoO}_3$  (10 nm)/Al(100 nm) is thermally evaporated in which the  $\text{C}_{60}$  interlayer is inserted to obtain Fermi level alignment between  $\text{MoO}_3$  and ICBA [21].

The interlayer-based contact engineering technique [21] allows us to inject holes directly from the top electrode into the HOMO of ICBA. For the case of an Ohmic contact on a trap-free, intrinsic semiconductor, the injected current is limited by space charge, as described by the Mott-Gurney square law, which is [22]

$$J = \frac{9}{8} \varepsilon \mu \frac{(V - V_{\text{bi}})^2}{L^3}, \quad (1)$$

where  $J$  is the current density,  $\varepsilon$  is the permittivity,  $\mu$  is the charge-carrier mobility,  $V$  is the voltage,  $V_{\text{bi}}$  is the built-in voltage due to asymmetric work functions of the electrodes [23], and  $L$  is the layer thickness. In Fig. 1(a), the measured hole-current density is plotted against voltage for three different layer thicknesses. Remarkably, the hole current depends on the square of the voltage and scales inversely with layer thickness to the third power, as demonstrated in Fig. 1(b), which is characteristic of a bulk trap-free

space-charge-limited current. This also confirms the formation of an Ohmic hole contact on ICBA. Furthermore, the hole-only devices do not show electroluminescence, confirming the absence of electron injection (see Appendix A). As a result, the current is carried by holes only. Because of the mismatch between the work function of PEDOT:PSS and the HOMO of ICBA, a small built-in voltage of approximately 0.45 V is present and the current in reverse bias is injection limited, as shown in Fig. 1(b). When fitting Eq. (1) to the forward  $J$ - $V$  characteristics, as shown in Fig. 1(a), a hole mobility of  $3 \times 10^{-3} \text{ cm}^2/\text{V s}$  is obtained for all layer thicknesses, using the experimentally determined relative permittivity of 3.9 [24]. This hole mobility is similarly high as the electron mobility in the ubiquitous fullerene derivative PCBM [25]. Interestingly, the ICBA bulk-hole mobility is even superior to that of typical hole-transport molecules and polymers [21,26–28].

To compare the hole transport directly to the electron transport, the electron current is measured in ICBA electron-only devices with an Al(35 nm)/ICBA/TPBi (5 nm)/Ba(5 nm)/Al(100 nm) structure, where TPBi [2,2',2'-(1,3,5-benzinetriyl)-tris(1-phenyl-1-H-benzimidazole)] is evaporated as a buffer layer. As can be observed in Fig. 1, the electron current is very similar to the hole current for a device with similar layer thickness. The electron mobility obtained by fitting the  $J$ - $V$  characteristics with Eq. (1) amounts to  $2.7 \times 10^{-3} \text{ cm}^2/\text{V s}$ , which is very close to the determined hole mobility.

Since Eq. (1) is a drift-only approximation, we also evaluate the electron and hole mobility with a numerical drift-diffusion solver [29] as shown in Appendix B. The drift-diffusion simulations can fit the full  $J$ - $V$  characteristics, simultaneously fitting the exponential diffusion current below the built-in voltage and the quadratic drift current above the built-in voltage. The built-in voltage is determined by both the barrier at the hole-extracting cathode and band bending at the Ohmic hole-injecting anode. The band bending typically amounts to approximately 0.3 eV for an Ohmic contact [23]. In the drift-diffusion simulations, the barrier at the cathode is determined to be about 0.75 eV, consistent with the difference between the ICBA HOMO (−5.9 eV) and the work function of PEDOT:PSS (5.1–5.2 eV). Combined with band bending, this barrier is also consistent with the built-in voltage of 0.45 V, as discussed in detail in Appendix B. For both electron- and hole-only devices, the thickness-dependent  $J$ - $V$  characteristics can be fitted with a mobility of  $2 \times 10^{-3}$  cm<sup>2</sup>/V s, without incorporating electron or hole traps. This mobility is slightly lower than the value estimated with Eq. (1), which does not consider the diffusion contribution to the current. The charge transport measurements demonstrate that ICBA is a material with balanced hole and electron transport, which has not been shown before for an organic semiconductor in a diode configuration.

To explore the charge transport in more detail and evaluate the energetic disorder, we investigate the temperature dependence of the hole and electron currents. The mobility in disordered semiconductors exhibiting hopping transport

depends on temperature, charge concentration, and electric field [19,30]. For a system with Gaussian disorder, these mobility characteristics can be described by the extended Gaussian disorder model (EGDM) [30], which uses three input parameters: the width of the density-of-states distribution  $\sigma$ , the lattice constant  $a$ , and a mobility prefactor  $\mu_\infty$ . The mobility prefactor determines the magnitude of the mobility,  $\sigma$  mainly controls its temperature and charge-concentration dependence, and  $a$  predominantly affects its field dependence. In the EGDM, the temperature-dependent mobility at zero field and density is a function of the energetic disorder and is given by [30]

$$\mu_0(T) = \mu_\infty c_1 \exp \left[ -c_2 \left( \frac{\sigma}{kT} \right)^2 \right], \quad (2)$$

with  $c_1 = 1.8 \times 10^{-9}$ ,  $c_2 = 0.42$ ,  $k$  is the Boltzmann constant, and  $T$  is the temperature. As can be seen from Eq. (2), the temperature dependence of the mobility at low fields and densities is controlled by two input parameters, viz. the mobility prefactor and the energetic disorder. To obtain the current density-voltage characteristics, the full EGDM mobility function, including the dependence on temperature, density, and field, is incorporated in the drift-diffusion solver [29].

Figure 2(a) shows the temperature-dependent current density-voltage characteristics of an ICBA hole-only device. The experimental data is fitted with drift-diffusion simulations incorporating the EGDM, using an energetic disorder  $\sigma$  of 0.10 eV and a lattice constant  $a$  of

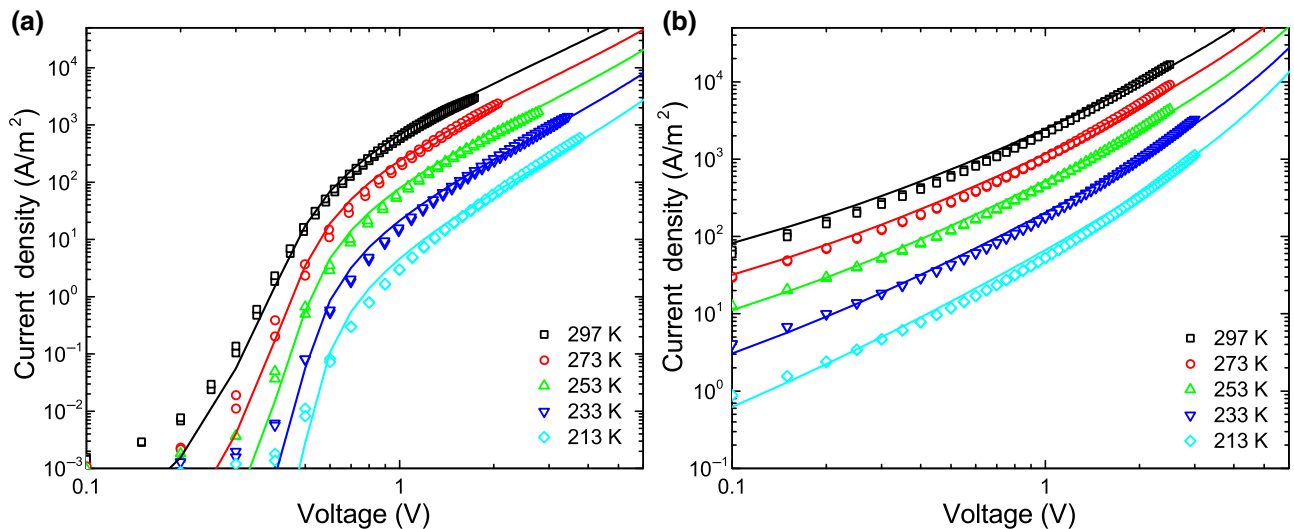


FIG. 2. Temperature-dependent current density-voltage characteristics of ICBA hole-only (a) and electron-only (b) devices, with ICBA layer thicknesses of 169 and 176 nm, respectively. Experimental data is plotted as symbols, the solid lines are fits with drift-diffusion simulations incorporating the temperature-, field-, and density-dependent mobility according to the EGDM. Due to the built-in voltage in the hole-only device, the steep diffusion-limited current is visible at low voltages [see Fig. 1(b)].

2 nm. The mobility for vanishing carrier density and electric field at room temperature,  $\mu_0$  (295 K), amounts to  $1.4 \times 10^{-3} \text{ cm}^2/\text{V s}$ . This number is slightly lower than the mobility extracted with Eq. (1) and from drift-diffusion simulations with a constant mobility, which is due to the presence of a nonzero space-charge density due to diffused carriers from the contacts of typically approximately  $10^{16} \text{ cm}^{-3}$  in the measurements [31]. We estimate the error in the energetic disorder to be within 0.01 eV, where higher or lower energetic disorder results in too strong or weak temperature dependence of the current density, respectively. We have checked that the measured temperature range falls within the validity window of the EGDM.

A similar analysis is performed for the electron transport, as shown in Fig. 2(b). The temperature-dependent  $J$ - $V$  characteristics are again fitted using the EGDM, yielding an energetic disorder  $\sigma$  of 0.09 eV and a lattice constant  $a$  of 3 nm. The electron mobility  $\mu_0$  (295 K) of  $1.4 \times 10^{-3} \text{ cm}^2/\text{V s}$  is very similar to the hole mobility, demonstrating balanced bipolar charge transport in ICBA, which is also reflected in the similar values obtained for the energetic disorder. The obtained charge-transport parameters are consistent for electron- and hole-only devices of different layer thicknesses (see Supplemental Material [24]).

The hole- and electron-transport simulations are performed without the need for incorporating additional trapping sites. Trap-free charge transport for both electrons and holes is quite exceptional in organic semiconductors, which frequently exhibit electron trapping [12,32–34]. While near-balanced charge transport in a poly(*p*-phenylene vinylene) derivative has been claimed [35], the thickness dependence of the current was not reported and parasitic hole injection from the used TiN bottom electrode in the electron-only device cannot be excluded [36]. Other studies have demonstrated highly unbalanced charge transport in this polymer [37,38]. As an exception to most conjugated polymers, trap-free electron and hole transport has been found in the copolymer N2200, however, hole transport was substantially inferior to electron transport due to highly unbalanced intrinsic mobilities [39]. The high and balanced bulk mobilities observed for ICBA are an experimental confirmation of the intrinsic bipolar character of organic semiconductors, which previously could only be assessed by deactivation of charge trapping either by doping [34,40], blending with an insulator [38], or by measuring at carrier densities much higher than the concentration of bulk traps [11].

The observation of balanced electron and hole transport in ICBA raises the question of whether a bipolar device can be fabricated in which electrons and holes are injected simultaneously. Bipolar injection, resulting in subsequent recombination, has been observed previously in devices of the fullerene derivative [60]PCBM with electrically detected magnetic resonance [41]. It has been observed by

Gadisa *et al.* that bipolar injection into a similar [60]PCBM device leads to electroluminescence [42]. Although these observations cannot evidence the presence of balanced electron and hole transport, they do support that bipolar injection and recombination are possible in fullerenes.

To confirm electron-hole recombination in ICBA, a bipolar device is fabricated in which an ICBA layer is sandwiched between a PEDOT:PSS bottom electrode and a TPBi(5 nm)/Ba/Al top electrode. The barrier at the non-Ohmic PEDOT:PSS electrode can be reduced by electrical conditioning in a bipolar device, enabling hole injection [43]. As observed in Fig. 3, the device exhibits electroluminescence, effectively operating as a light-emitting diode. The measured light output shows the presence of both electrons and holes in the device. In the hole-only device, that is, under unipolar injection conditions, electroluminescence cannot be detected (see Appendix A). The external quantum efficiency for electroluminescence in the bipolar device is determined to be  $1.8 \times 10^{-5}$ , which indicates relatively efficient electron-hole recombination when considering the low-fluorescence quantum yield of fullerenes (approximately  $7 \times 10^{-5}$  for  $\text{C}_{60}$  films at 300 K [44]).

In conclusion, trap-free space-charge-limited hole currents are measured in the fullerene derivative ICBA. The determined bulk hole mobility of  $1.4 \times 10^{-3} \text{ cm}^2/\text{V s}$  at zero field is equally as high as the bulk electron mobility, and similar to the electron mobility of the widely-used fullerene derivative PCBM, highlighting the fact that fullerenes can be excellent hole-transporting materials. Both the electron and hole transport exhibit trap-free characteristics, resulting in the unique observation of an organic semiconductor with trap-free and balanced electron and hole transport.

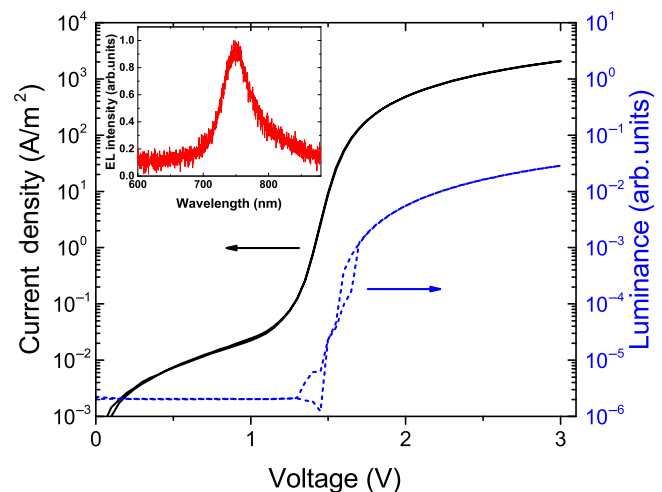


FIG. 3. Current density and luminance vs voltage for an ICBA organic light-emitting diode (OLED) with an ICBA layer thickness of 118 nm. The electroluminescence spectrum is shown in the inset. EL, electroluminescence.

## ACKNOWLEDGMENTS

This project has received funding from the European Union Horizon 2020 research and innovation programme under Grant Agreement No. 646176 (EXTMOS).

## APPENDIX A: CONFIRMATION OF HOLE-ONLY CURRENT

In Fig. 4, it is demonstrated that the current measured in the hole-only devices is carried by holes only and electron injection is absent. This can be confirmed by performing electroluminescence measurements, which we detect as a photocurrent from a silicon photodiode. Figure 4 demonstrates that while electroluminescence is observed in the bipolar device above the built-in voltage following the injected current, there is no electroluminescence detected for the hole-only device, despite the large current density. This implies that electron injection from PEDOT:PSS in the hole-only device is not significant, confirming that the measured current is carried by holes only. In addition, Fig. 4 shows the current of the bipolar device in reverse bias. Only a leakage current is observed in reverse bias, demonstrating that electron injection from PEDOT:PSS and hole injection from TPBi/Ba/Al are not significant. As a result, electroluminescence is also absent in reverse bias. The low built-in voltage in the hole-only device once more confirms the unipolar character.

## APPENDIX B: DRIFT-DIFFUSION SIMULATIONS WITH A CONSTANT MOBILITY

As discussed in Ref. [23], the current density in an asymmetric single-carrier device can be described by a diffusion-dominated current below the built-in voltage and

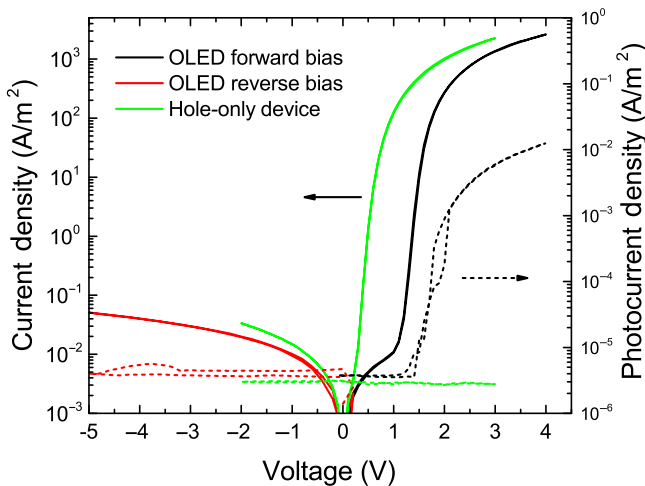


FIG. 4. Current density (solid lines) and light output (dashed lines) vs voltage for hole-only and bipolar (OLED) devices of ICBA. The light output is measured as a photocurrent by a silicon photodiode.

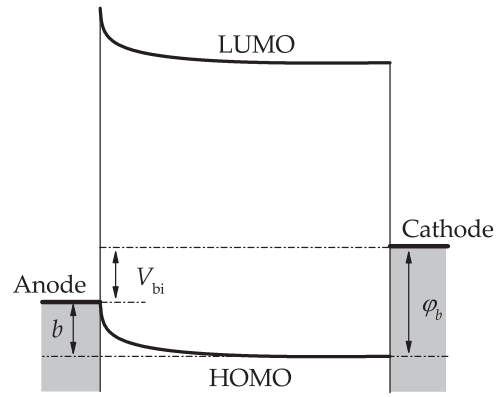


FIG. 5. Schematic band diagram of an ICBA hole-only device with an Ohmic hole-injecting anode and a non-Ohmic hole-extracting cathode at the built-in voltage ( $V = V_{bi}$ ).

a drift-dominated current above the built-in voltage. As illustrated in the energy band diagram in Fig. 5, the built-in voltage in a hole-only device can be described as the potential difference between the energetic barrier at the cathode  $\phi_b$ , and the band-bending parameter  $b$ . Band bending is present at the Ohmic contact, which is the result of charges diffusing into the organic-semiconductor layer. The band-bending parameter  $b$  typically has a value of approximately 0.3 V and can be calculated as described in Ref. [23].

Figure 6(a) shows the experimental data and the simulated drift-diffusion current for hole-only devices of different ICBA layer thicknesses. A constant mobility of  $2.0 \times 10^{-3} \text{ m}^2/\text{V s}$  is used for all layer thicknesses. The barrier at the injecting contact is set to 0 V (Ohmic contact). The barrier at the extracting (PEDOT:PSS) contact  $\phi_b$  (see Fig. 5), which shifts the simulated curves horizontally along the voltage axis, is tuned to fit the exponential diffusion regime below  $V_{bi}$ . The values obtained for  $\phi_b$  are 0.72, 0.78, and 0.78 V for layer thicknesses of 75, 120, and 169 nm, respectively. The variation in the barrier  $\phi_b$  is small and the value is consistent with the difference between the ICBA HOMO ( $-5.9 \text{ eV}$ ) and the work function of PEDOT:PSS ( $5.1\text{--}5.2 \text{ eV}$ ). Since  $V_{bi} = \phi_b - b$ , as shown schematically in Fig. 5, the value of the cathode barrier  $\phi_b$  is in agreement with the built-in voltage in Fig. 1, considering a typical band-bending parameter  $b$  of approximately 0.3 V [23].

Figure 6(b) shows the current density-voltage characteristics of ICBA electron-only devices and corresponding fits with drift-diffusion simulations. A constant mobility of  $2.0 \times 10^{-3} \text{ m}^2/\text{V s}$  is used for both layer thicknesses. The deviation at higher voltage is due to the field dependence of the mobility, not included in this simulation. The simulations are performed without injection barrier and the barrier at the extracting contact  $\phi_b$  is 0.25 V, thus a built-in voltage is consequently absent. The small barrier  $\phi_b$  results in a slightly injection-limited current in reverse bias.

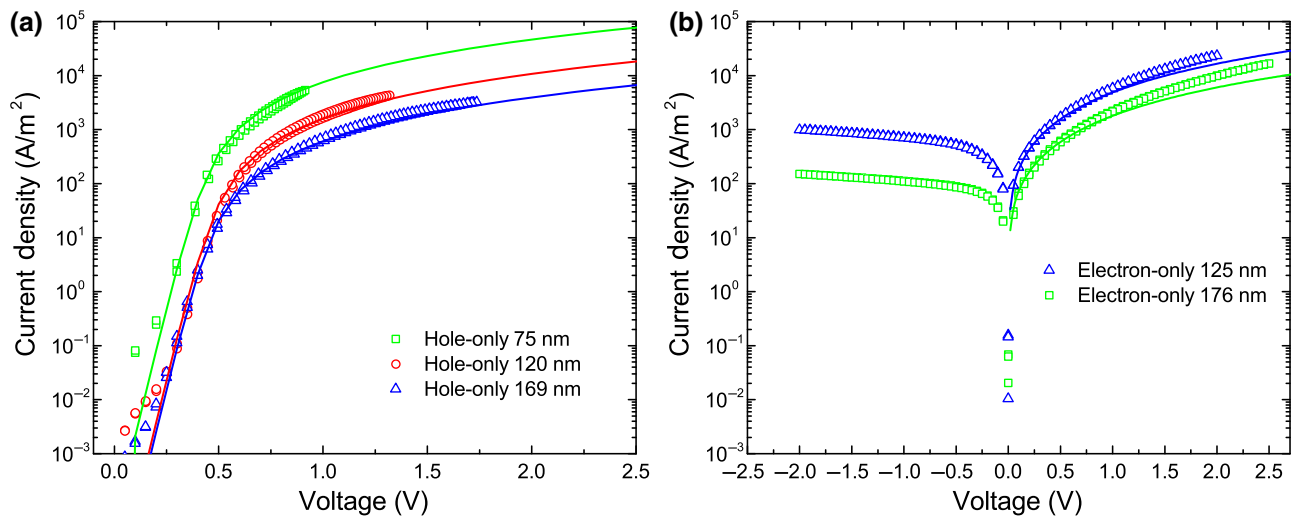


FIG. 6. Current density-voltage characteristics of ICBA hole-only (a) and electron-only (b) devices of different layer thicknesses. The symbols represent experimental data, the lines are fits with drift-diffusion simulations using a constant mobility.

- [1] J. E. Anthony, A. Facchetti, M. Heeney, S. R. Marder, and X. Zhan, n-Type organic semiconductors in organic electronics, *Adv. Mater.* **22**, 3876 (2010).
- [2] J. Liu, L. Qiu, G. Portale, M. Koopmans, G. ten Brink, J. C. Hummelen, and L. J. A. Koster, n-Type organic thermoelectrics: improved power factor by tailoring host-dopant miscibility, *Adv. Mater.* **29**, 1701641 (2017).
- [3] G. Yang, H. Tao, P. Qin, W. Ke, and G. Fang, Recent progress in electron transport layers for efficient perovskite solar cells, *J. Mater. Chem. A* **4**, 3970 (2016).
- [4] G. Yu, J. Gao, J. C. Hummelen, F. Wudl, and A. J. Heeger, Polymer photovoltaic cells: enhanced efficiencies via a network of internal donor-acceptor heterojunctions, *Science* **270**, 1789 (1995).
- [5] M. Lenes, G. A. H. Wetzelaer, F. B. Kooistra, S. C. Veenstra, J. C. Hummelen, and P. W. M. Blom, Fullerene bisadducts for enhanced open-circuit voltages and efficiencies in polymer solar cells, *Adv. Mater.* **20**, 2116 (2008).
- [6] Y. He, H.-Y. Chen, J. Hou, and Y. Li, Indene-C<sub>60</sub> bisadduct: A new acceptor for high-performance polymer solar cells, *J. Am. Chem. Soc.* **132**, 1377 (2010).
- [7] H. Li, B. C.-K. Tee, J. J. Cha, Y. Cui, J. W. Chung, S. Y. Lee, and Z. Bao, High-mobility field-effect transistors from large-area solution-grown aligned C<sub>60</sub> single crystals, *J. Am. Chem. Soc.* **134**, 2760 (2012).
- [8] Q. Burlingame, C. Coburn, X. Che, A. Panda, Y. Qu, and S. R. Forrest, Centimetre-scale electron diffusion in photoactive organic heterostructures, *Nature* **554**, 77 (2018).
- [9] C. Jehoulet, A. J. Bard, and F. Wudl, Electrochemical reduction and oxidation of C<sub>60</sub> films, *J. Am. Chem. Soc.* **113**, 5456 (1991).
- [10] V. Coropceanu, J. Cornil, D. A. da Silva Filho, Y. Olivier, R. Silbey, and J.-L. Brédas, Charge transport in organic semiconductors, *Chem. Rev.* **107**, 926 (2007).
- [11] L. L. Chua, J. Zaumseil, J. F. Chang, E. C. W. Ou, P. K. H. Ho, H. Sirringhaus, and R. H. Friend, General observation of n-type field-effect behaviour in organic semiconductors, *Nature* **434**, 194 (2005).
- [12] H. T. Nicolai, M. Kuik, G. A. H. Wetzelaer, B. de Boer, C. Campbell, C. Risko, J. L. Brédas, and P. W. M. Blom, Unification of trap-limited electron transport in semiconducting polymers, *Nat. Mater.* **11**, 882 (2012).
- [13] E. Frankevich, Y. Maruyama, and H. Ogata, Mobility of charge carriers in vapor-phase grown C<sub>60</sub> single crystal, *Chem. Phys. Lett.* **214**, 39 (1993).
- [14] C. Li, L. Duan, H. Li, and Y. Qiu, Universal trap effect in carrier transport of disordered organic semiconductors: Transition from shallow trapping to deep trapping, *J. Phys. Chem. C* **118**, 10651 (2014).
- [15] R. Könenkamp, G. Priebe, and B. Pietzak, Carrier mobilities and influence of oxygen in C<sub>60</sub> films, *Phys. Rev. B* **60**, 11804 (1999).
- [16] J. Mort, M. Machonkin, R. Ziolo, and I. Chen, Electronic carrier transport and photogeneration in buckminsterfullerene films, *Appl. Phys. Lett.* **61**, 1829 (1992).
- [17] D. Sarkar and N. J. Halas, Dember effect in C<sub>60</sub> thin films, *Solid State Commun.* **90**, 261 (1994).
- [18] T. D. Anthopoulos, C. Tanase, S. Setayesh, E. J. Meijer, J. C. Hummelen, P. W. M. Blom, and D. M. de Leeuw, Ambipolar organic field-effect transistors based on a solution-processed methanofullerene, *Adv. Mater.* **16**, 2174 (2004).
- [19] C. Tanase, E. J. Meijer, P. W. M. Blom, and D. M. de Leeuw, Unification of the Hole Transport in Polymeric Field-Effect Transistors and Light-Emitting Diodes, *Phys. Rev. Lett.* **91**, 216601 (2003).
- [20] A. Armin, S. Shoaee, Q. Lin, P. L. Burn, and P. Meredith, On the unipolarity of charge transport in methanofullerene diodes, *npj Flexible Electronics* **1**, 13 (2017).
- [21] N. B. Kotadiya, H. Lu, A. Mondal, Y. Ie, D. Andrienko, P. W. M. Blom, and G. A. H. Wetzelaer, Universal strategy

- for Ohmic hole injection into organic semiconductors with high ionization energies, *Nat. Mater.* **17**, 329 (2018).
- [22] N. F. Mott and R. W. Gurney, *Electronic Processes in Ionic Crystals* (Oxford University Press, London, 1940).
- [23] P. de Bruyn, A. H. P. van Rest, G. A. H. Wetzelaer, D. M. de Leeuw, and P. W. M. Blom, Diffusion-Limited Current in Organic Metal-Insulator-Metal Diodes, *Phys. Rev. Lett.* **111**, 186801 (2013).
- [24] See Supplemental Material at <http://link.aps.org/supplemental/10.1103/PhysRevApplied.11.024069> for additional simulations and measurement of the relative permittivity.
- [25] V. D. Mihailetschi, J. K. J. van Duren, P. W. M. Blom, J. C. Hummelen, R. A. J. Janssen, J. M. Kroon, M. T. Rispens, W. J. H. Verhees, and M. M. Wienk, Electron transport in a methanofullerene, *Adv. Funct. Mater.* **13**, 43 (2003).
- [26] S. Logan, J. E. Donaghey, W. Zhang, I. McCulloch, and A. J. Campbell, Compatibility of amorphous triarylamine copolymers with solution-processed hole injecting metal oxide bottom contacts, *J. Mater. Chem. C* **3**, 4530 (2015).
- [27] B. Ebenhoch, S. A. J. Thomson, K. Genevičius, G. Juška, and I. D. W. Samuel, Charge carrier mobility of the organic photovoltaic materials PTB7 and PC<sub>71</sub>BM and its influence on device performance, *Org. Electron.* **22**, 62 (2015).
- [28] D. B. Shinde, J. K. Salunke, N. R. Candeias, F. Tinti, M. Gazzano, P. P. Wadgaonkar, A. Priimagi, N. Camaioni, and P. Vivo, Crystallisation-enhanced bulk hole mobility in phenothiazine-based organic semiconductors, *Sci. Rep.* **7**, 46268 (2017).
- [29] L. J. A. Koster, E. C. P. Smits, V. D. Mihailetschi, and P. W. M. Blom, Device model for the operation of polymer/fullerene bulk heterojunction solar cells, *Phys. Rev. B* **72**, 085205 (2005).
- [30] W. F. Pasveer, J. Cottaar, C. Tanase, R. Coehoorn, P. A. Bobbert, P. W. M. Blom, D. M. de Leeuw, and M. A. J. Michels, Unified Description of Charge-Carrier Mobilities in Disordered Semiconducting Polymers, *Phys. Rev. Lett.* **94**, 206601 (2005).
- [31] N. I. Craciun, J. J. Brondijk, and P. W. M. Blom, Diffusion-enhanced hole transport in thin polymer light-emitting diodes, *Phys. Rev. B* **77**, 035206 (2008); G. A. H. Wetzelaer and P. W. M. Blom, Ohmic current in organic metal-insulator-metal diodes revisited, *Phys. Rev. B* **89**, 241201 (2014).
- [32] R. Steyrlauthner, S. Bange, and D. Neher, Reliable electron-only devices and electron transport in n-type polymers, *J. Appl. Phys.* **105**, 064509 (2009).
- [33] M. Mesta, M. Carvelli, R. J. de Vries, H. van Eersel, J. J. M. van der Holst, M. Schober, M. Furno, B. Lüsse, K. Leo, P. Loebel, R. Coehoorn, and P. A. Bobbert, Molecular-scale simulation of electroluminescence in a multilayer white organic light-emitting diode, *Nat. Mater.* **12**, 652 (2013).
- [34] B. D. Naab, S. Himmelberger, Y. Diao, K. Vandewal, P. Wei, B. Lussem, A. Salleo, and Z. Bao, High mobility N-type transistors based on solution-sheared doped 6,13-bis(triisopropylsilyl)ethynylpentacene thin films, *Adv. Mater.* **25**, 4663 (2013).
- [35] L. Bozano, S. A. Carter, J. C. Scott, G. G. Malliaras, and P. J. Brock, Temperature- and field-dependent electron and hole mobilities in polymer light-emitting diodes, *Appl. Phys. Lett.* **74**, 1132 (1999).
- [36] M. M. Mandoc, B. de Boer, and P. W. M. Blom, Electron-only diodes of poly(dialkoxy-p-phenylene vinylene) using hole-blocking bottom electrodes, *Phys. Rev. B* **73**, 155205 (2006).
- [37] B. K. Crone, I. H. Campbell, P. S. Davids, and D. L. Smith, Charge injection and transport in single-layer organic light-emitting diodes, *Appl. Phys. Lett.* **73**, 3162 (1998).
- [38] D. Abbaszadeh, A. Kunz, G. A. H. Wetzelaer, J. J. Michels, N. I. Craciun, K. Koynov, I. Lieberwirth, and P. W. M. Blom, Elimination of charge carrier trapping in diluted semiconductors, *Nat. Mater.* **15**, 628 (2016).
- [39] G. A. H. Wetzelaer, M. Kuik, Y. Olivier, V. Lemaire, J. Cornil, S. Fabiano, M. A. Loi, and P. W. M. Blom, Asymmetric electron and hole transport in a high-mobility n-type conjugated polymer, *Phys. Rev. B* **86**, 165203 (2012).
- [40] Y. Zhang, B. de Boer, and P. W. M. Blom, Trap-free electron transport in poly(p-phenylene vinylene) by deactivation of traps with n-type doping, *Phys. Rev. B* **81**, 085201 (2010).
- [41] H. Morishita, W. J. Baker, D. P. Waters, R. Baarda, J. M. Lupton, and C. Boehme, Mechanisms of spin-dependent dark conductivity in films of a soluble fullerene derivative under bipolar injection, *Phys. Rev. B* **89**, 125311 (2014).
- [42] A. Gadisa, K. Tvingstedt, K. Vandewal, F. Zhang, J. V. Manca, and O. Inganäs, Bipolar charge transport in fullerene molecules in a bilayer and blend of polyfluorene copolymer and fullerene, *Adv. Mater.* **22**, 1008 (2010).
- [43] D. Poplavskyy, J. Nelson, and D. D. C. Bradley, Ohmic hole injection in poly(9,9-dioctylfluorene) polymer light-emitting diodes, *Appl. Phys. Lett.* **83**, 707 (2003).
- [44] D. R. Haynes, A. Tokmakoff, and S. M. George, Temperature-dependent absolute fluorescence quantum yield of C<sub>60</sub> multilayers, *Chem. Phys. Lett.* **214**, 50 (1993).